

1 **INFLAMMATORY CELLULAR RESPONSE TO MECHANICAL VENTILATION IN**
2 **ELASTASE-INDUCED EXPERIMENTAL EMPHYSEMA: ROLE OF PRE-EXISTING**
3 **ALVEOLAR MACROPHAGES INFILTRATION**

4

5 Anahita ROUZE^{1,2}, MD, Guillaume VOIRIOT^{1,3}, MD, Elise GUIVARCH¹, MD, Françoise ROUX¹,
6 MD, Jeanne TRAN VAN NHIEU^{3,4}, MD, PhD, Daniel ISABEY^{1,3}, PhD, Laurent BROCHARD⁵, MD,
7 PhD, Bernard MAITRE^{1,3,6,7}, MD, PhD, Armand MEKONTSO-DESSAP^{1,3,6}, MD, PhD, Jorge
8 BOCZKOWSKI^{1,3,6}, MD, PhD.

9

10 ¹INSERM, Unité U955 (Institut Mondor de Recherche Biomédicale), Créteil, 94010 France

11 ²CHU Lille, Centre de Réanimation, F-59000 Lille, France

12 ³Université Paris Est Créteil Val de Marne, Faculté de Médecine, Groupe de recherche clinique
13 CARMAS, Créteil, 94010 France

14 ⁴AP-HP, Hôpitaux Universitaires Henri Mondor, Département de Pathologie, Créteil, 94010 France

15 ⁵Interdepartmental Division of Critical Care Medicine, St Michael's Hospital, Toronto, ON, Canada

16 ⁶AP-HP, Hôpitaux Universitaires Henri Mondor, DHU A-TVB, Service de Réanimation Médicale,
17 Créteil, 94010 France

18 ⁷Centre Hospitalier Intercommunal de Créteil, Service de Pneumologie et Pathologie Professionnelle,
19 Créteil, 94010, France

20

21 **Email adresses of all co-authors :** guillaumevoiriot@hotmail.com, elise.guivarch@gmail.com,
22 francoise.roux@oniris-nantes.fr, jeanne.tran-van-nhieu@aphp.fr, daniel.isabey@inserm.fr,
23 BrochardL@smh.ca, bm.maitre@gmail.com, armand.dessap@gmail.com,
24 jorge.boczowski@inserm.fr

25

26 **CORRESPONDING AUTHOR**

27 Dr Anahita Rouzé

28 Centre de Réanimation, CHU Lille, Boulevard du Pr Leclercq, F-59000 Lille, France

29 phone: (0033) 3 20 44 40 84

30 fax : (0033) 3 20 44 50 94

31 e-mail: anahita.rouze@chru-lille.fr

32

33 **WORD COUNT FOR THE ABSTRACT:** 349

34 **WORD COUNT FOR THE MANUSCRIPT:** 2466

35

36 **ABSTRACT**

37 **Background**

38 An excessive pulmonary inflammatory response could explain the poor prognosis of chronic
39 obstructive pulmonary disease (COPD) patients submitted to invasive mechanical ventilation. The aim
40 of this study was to evaluate the response to normal tidal volume (V_t) mechanical ventilation in a
41 murine model of pulmonary emphysema, which represents the alveolar component of COPD. In this
42 model, two time points associated with different levels of lung inflammation but similar lung
43 destruction, were analyzed.

44 **Methods**

45 C57BL/6 mice received a tracheal instillation of 5 IU of porcine pancreatic elastase (Elastase mice) or
46 the same volume of saline (Saline mice). Fourteen (D14) and 21 (D21) days after instillation, mice
47 were anesthetized, intubated, and either mechanically ventilated (MV) with a normal V_t (8 mL/kg) or
48 maintained on spontaneous ventilation (SV) during two hours. We analyzed respiratory mechanics,
49 emphysema degree (mean chord length by lung histological analysis), and lung inflammation

50 (bronchoalveolar lavage (BAL) cellularity, proportion and activation of total lung inflammatory cells
51 by flow cytometry).

52 **Results**

53 As compared with Saline mice, Elastase mice showed a similarly increased mean chord length and
54 pulmonary compliance at D14 and D21, while BAL cellularity was comparable between groups. Lung
55 mechanics was similarly altered during mechanical ventilation in Elastase and Saline mice. Activated
56 alveolar macrophages *CD11b^{mid}* were present in lung parenchyma in both Elastase SV mice and
57 Elastase MV mice at D14 but were absent at D21 and in Saline mice, indicating an inflammatory state
58 with elastase at D14 only. At D14, Elastase MV mice showed a significant increase in percentage of
59 neutrophils concomitant with a decrease in percentage of alveolar macrophages in total lung, as
60 compared with Elastase SV mice. Furthermore, alveolar macrophages of Elastase MV mice at D14
61 overexpressed Gr1, and monocytes showed a trend to overexpression of CD62L, compared with
62 Elastase SV mice.

63 **Conclusions**

64 In an elastase-induced model of pulmonary emphysema, normal Vt mechanical ventilation produced
65 an increase in the proportion of pulmonary neutrophils, and an activation of alveolar macrophages and
66 pulmonary monocytes. This response was observed only when the emphysema model showed an
67 underlying inflammation (D14), reflected by the presence of activated alveolar macrophages
68 *CD11b^{mid}*.

69

70 **KEYWORDS**

71 alveolar macrophages, elastase, flow cytometry, mechanical ventilation, mice, pulmonary emphysema

72

73 **MAIN TEXT**

74

75 **BACKGROUND**

76

77 Chronic obstructive pulmonary disease (COPD) is characterized by persistent airflow limitation,
78 associated with an excessive inflammatory response to noxious particles or gases in the airways and
79 the lung (1). Invasive mechanical ventilation may lead to a higher mortality rate in this population (2),
80 and has been recognized as an independent risk factor for mortality among COPD patients admitted to
81 intensive care units (ICU) with acute respiratory failure (3).

82 Numerous experimental and clinical studies have reported the concept of ventilator-induced lung
83 injury (VILI) (4–8). The use of high tidal volumes (V_t) is one of its main contributors, especially
84 leading to an acute inflammation secondary to lung overdistension, and known as “biotrauma” (9–13).
85 Normal V_t , close to 8 mL/kg may also lead to pulmonary inflammation (12,14,15). Furthermore, a
86 preexisting lung inflammatory process could aggravate the inflammatory response to mechanical
87 ventilation (12,16).

88 Since chronic airway and lung inflammation plays a major role in the pathogenesis of COPD, and its
89 alveolar component, emphysema (17–19), we hypothesized that mechanical ventilation may aggravate
90 preexisting pulmonary inflammation in emphysematous lungs. This phenomenon could explain, at
91 least in part, the detrimental effect of invasive mechanical ventilation in COPD patients. The aim of
92 our study was therefore to evaluate the inflammatory response during two hours of normal V_t
93 mechanical ventilation in a murine model of pulmonary emphysema induced by elastase (20). This
94 model is characterized by an early and transient alveolar infiltration by macrophages (21–23).
95 Thereby, in order to examine the effects of pre-existing alveolar macrophages infiltration in the
96 inflammatory response to mechanical ventilation, animals were examined at days 14 and 21 after
97 elastase instillation, two time points associated with similar lung destruction, but the presence and the
98 absence of macrophages infiltration, respectively.

99

100 **METHODS**

101

102 Additional details on the methods are provided in an additional file.

103

104 **Animal model**

105 All the experiments were performed in accordance with the official regulations of the French Ministry
106 of Agriculture and the US National Institute of Health guidelines for the experimental use of animals;
107 and were approved by the local institutional animal care and use committee. Six-weeks-old male
108 C57BL/6 mice (Janvier Labs, Le Genest Saint-Isle, France) received the instillation of either 5 IU of
109 porcine pancreatic elastase (Elastin Products, Owensville, MO, USA) (Elastase mice), or 50 μ l of
110 saline (Saline mice) into the trachea (23). Mice were then subjected to subsequent ventilation at two
111 time points, 14 and 21 days after instillation.

112

113 **Mechanical ventilation**

114 Mice were anesthetized and intubated. Mice in mechanical ventilation (MV) group were ventilated for
115 two hours by means of a computer-driven small-animal ventilator (*FlexiVent*, Scireq, Montreal,
116 Canada) as follows: $V_t = 8 \mu\text{L/g}$ of body weight, respiratory rate = 180 /min, end-expiratory pressure
117 = 1.5 cmH_2O , and fraction of inspired oxygen = 0.4 - 0.6 (24). A control group (SV) consisted of
118 anesthetized, intubated mice, maintained on spontaneous ventilation for two hours.

119

120 **Experimental design**

121 The experimental design included four groups, at two distinct time points from tracheal instillation
122 (D14 and D21) (figure 1): Saline SV (saline instillation followed by spontaneous ventilation), Elastase
123 SV (elastase instillation followed by spontaneous ventilation), Saline MV (saline instillation followed

124 by mechanical ventilation), and Elastase MV (elastase instillation followed by mechanical
125 ventilation).

126

127 **Respiratory mechanics**

128 The *flexiVent* ventilator was used for continuous measurement of mean and peak airway pressures
129 (Ppeak, Pmean) and to explore the respiratory mechanics using different waveforms (24). Single
130 frequency forced oscillation techniques were assessed at initiation of mechanical ventilation, before
131 (H0) and after (H0') volume history standardization, and then repeated hourly (H1 and H2), for
132 calculation of respiratory system dynamic resistance and compliance.

133

134 **Specimen collection**

135 After sacrifice, bronchoalveolar lavage (BAL) was performed, lungs were collected for either fixation
136 (4% paraformaldehyde) and paraffin embedding, or flow cytometric analysis.

137

138 **Morphometric analysis**

139 Sections of 5 μm thickness of the left lung were stained with hematoxylin and eosin. Fifteen digital
140 photomicrographs were acquired at x200 magnification in a systematic fashion (Axioplan 2
141 microscope equipped with an MRc digital color camera (Zeiss, Oberkochen, Germany)). Emphysema
142 was quantified by measurement of alveolar diameters with an image analysis software (ImageJ, NIH,
143 Bethesda, USA). This automated analysis was made vertically and horizontally on each
144 photomicrograph. The mean chord length of alveoli was obtained by averaging those measurements
145 (23).

146

147 **Bronchoalveolar lavage**

148 The total cell count of BAL was determined using a Malassez hemocytometer (Hycor biomedical,
149 Indianapolis, IN, USA). Differential cell counts were done on cytocentrifuge preparations (Cytospin3;
150 Shandon Scientific, Cheshire, UK) stained with Diff-Quick stain (Baxter Diagnostics, McGaw Park,
151 IL, USA).

152

153 **Flow cytometric analysis**

154 Mechanical disruption followed by enzymatic digestion of murine lungs were performed (11,25).
155 Total lung cell suspensions were obtained, stained with fluorochrome-conjugated anti-mouse
156 antibodies for CD11b, CD11c, Gr1 (Ly6C/G), F4/80 and CD62L (L-selectin) or appropriate isotype-
157 matched controls, and analysed using a 7 channel cytometer (CyAn ADP Analyser, Beckman Coulter,
158 Brea, USA) with Summit software (Summit v4.3, Dako, Cambridge, UK). Three inflammatory cell
159 populations in murine lung were identified (figure 2). CD11b-, CD11c+ phenotype, with high
160 autofluorescence defined alveolar macrophages (figure 2C) (25). Monocytes and neutrophils were
161 identified as CD11b+, CD11c- cells but differed especially in their granularity (side-scatter, SS), and
162 F4/80 and Gr1 expression (11,12). High SS and F4/80-, Gr1+ phenotype defined neutrophils, whereas
163 low SS, and F4/80+, Gr1^{mid} phenotype characterized monocytes (figures 2D, 2E, 2F). Cells
164 activation state was assessed using expression of CD62L and CD11b adhesion molecule, as well as
165 Gr1. All flow cytometric results were presented as relative values, called percentage of gated cells
166 (26).

167

168 **Statistical analysis**

169 Data were analyzed using SPSS Base 16.0 statistical software (SPSS Inc, Chicago, IL, USA).
170 Continuous data were expressed as median \pm interquartile range. Independent sample were compared
171 using Kruskal-Wallis test followed by pairwise Mann-Whitney test, with correction for multiple

172 testing by Benjamini-Hochberg false discovery rate. Two-tailed p values smaller than 0.10 and 0.05
173 were considered marginally significant and significant respectively.

174

175 **RESULTS**

176

177 Additional tables and figures are provided in additional file.

178

179 **Elastase-induced emphysema model**

180 Morphometric analysis showed a marked increase in mean chord length in Elastase mice (at both D14
181 and D21) as compared to Saline mice (Figure 3, Table S3 in additional file). Elastase mice (at both
182 D14 and D21) also exhibited higher values of respiratory system dynamic compliance at the
183 beginning of mechanical ventilation (after volume history standardisation), as compared to Saline
184 mice (Table 1, Figure 4).

185 BAL cellularity was similar between Saline and Elastase mice, at both D14 and D21 (Table S4 in
186 additional file) and differential cell count showed a predominance of macrophages (>90% of total
187 cells) in all groups. Flow cytometric analysis of inflammatory cells from total lung cell suspensions
188 found a marginally significant increase in the percentage of alveolar macrophages in Elastase SV mice
189 compared with Saline SV mice at D14 (Figure 5). These macrophages showed a trend towards an
190 overexpression of CD11b and a stronger autofluorescence, compared with Saline SV mice (Figure 6).
191 Flow cytometric analyses were similar between Elastase SV and Saline SV mice at D21, except for a
192 significant increase in autofluorescence of alveolar macrophages in the former group (Figure S1 and
193 S2 in additional file).

194

195 **Effect of mechanical ventilation**

196 A gradual decrease in respiratory system compliance (with associated increase in peak airway
197 pressures) was observed in both Elastase MV and Saline MV mice during the two hours of
198 mechanical ventilation. This decrease was similar between Elastase MV and Saline MV mice at D14,
199 but was greater in the former group at D21 (40.8% *versus* 34.3%, $p < 0.05$, Table 1, Figure 4).
200 BAL cellularity was comparable between Elastase MV, Elastase SV, Saline MV and Saline SV mice,
201 at both D14 and D21 time points (Table S4 in additional file). Flow cytometric analysis on total lung
202 cell suspensions did not find any significant change in pulmonary inflammatory cell populations or
203 cellular activation state between Saline MV and Saline SV mice, but with a trend towards increased
204 percentage of neutrophils and increased CD62L expression on monocytes in the former group (Figure
205 5 and 6B).
206 A significant decrease in the percentage of alveolar macrophages (with a concomitant increase in the
207 percentage of neutrophils) was noted at D14 in Elastase MV mice as compared to Elastase SV mice
208 (Figure 5). This was associated with a change in alveolar macrophages phenotype, with a marginally
209 significant overexpression of Gr1 in the former group (Figure 6A). Pulmonary monocytes also
210 exhibited a modified phenotype, with a maximal expression of CD62L in Elastase MV mice (Figure
211 6B). A particular stairs aspect was observed in CD62L expression on monocytes, which gradually
212 increased in relation to the successive assaults between Saline SV, Elastase SV, Saline MV and
213 Elastase MV groups. All above mentioned flow cytometry differences were not observed at D21 time
214 point, except for a stronger autofluorescence of alveolar macrophages in Elastase MV mice as
215 compared to Saline MV mice, which was present both at D14 and D21 (Figure S1 and S2 in additional
216 file).

217

218 **DISCUSSION**

219

220 Main results of our study are as follows: i) elastase instillation resulted in a similarly increased mean
221 chord length and respiratory system compliance at D14 and D21, as compared to saline instillation; ii)
222 these alterations were associated with a transient lung infiltration (only at D14) of activated alveolar
223 macrophages *CD11b^{mid}*; iii) lung mechanics was similarly altered during a two hours mechanical
224 ventilation in Elastase and Saline mice, with a gradual decrease in respiratory system compliance; iv)
225 at D14, mechanically ventilated Elastase mice showed a significant increase in the percentage of
226 neutrophils concomitant with a decrease in the percentage of alveolar macrophages in total lung,
227 compared with Elastase animals spontaneously ventilating. Furthermore, alveolar macrophages of
228 mechanically ventilated Elastase mice at D14 overexpressed Gr1, whereas monocytes showed a trend
229 to overexpression of CD62L.

230 Elastase-induced emphysema model has been described in numerous studies (20–23,27). Murine
231 lungs undergo an intense inflammatory reaction within the first week after elastase instillation, then
232 show a minimal inflammation state in the late phase, after D21. This situation mimics what is
233 observed in human emphysematous lung (17). Moreover, we used a dose of elastase inducing a degree
234 of emphysema similar to that observed after cigarette smoke exposure (near 30% increase in mean
235 chord length) (28). Time course of histological emphysema and alveolar macrophages infiltration
236 observed only at D14 in Elastase SV animals is consistent with previous data from the literature (21–
237 23,27). To our knowledge, our study is the first to provide phenotypic characterization of alveolar
238 macrophages in elastase model, by showing overexpression of CD11b in these cells at D14. These
239 macrophages are similar in their phenotype to pulmonary interstitial macrophages (25,29), but their
240 strong autofluorescence identifies them as alveolar macrophages. CD11b is an adhesion molecule
241 whose expression reflects the level of activation of various inflammatory cells. Activated alveolar
242 macrophages play a central role in the pathophysiology of pulmonary emphysema in mice and humans
243 (30). An increased expression of CD11b has been reported on macrophages collected in induced
244 sputum of COPD patients. Interestingly, CD11b expression intensity was correlated with the severity

245 of airflow limitation (31). High autofluorescence of alveolar macrophages, as observed in Elastase
246 mice (in either SV or MV groups, at both instillation times), has been previously reported in the BAL
247 of smokers (32). A link with tobacco particles phagocytosis has been suggested, without clear
248 biological significance.

249 We chose normal Vt strategy for its clinical relevance, as Vt close to 8 ml/kg are now widespread in
250 most mechanically ventilated patients (33). In terms of respiratory mechanics, both D14 and D21
251 Elastase mice responded to mechanical ventilation similarly to Saline mice, decreasing to the same
252 extent their respiratory system compliance within two hours of ventilation. This decrease is reported
253 in various ventilated murine models and results from progressive alveolar derecruitment (34). An
254 identical mechanical response to normal Vt mechanical ventilation has been observed in a TIMP3 KO
255 murine model of emphysema (35). Following two hours of normal Vt mechanical ventilation, we
256 observed a significant increase in the percentage of neutrophils concomitant with decrease in the
257 percentage of alveolar macrophages only in D14 Elastase mice. Neutrophils recruitment to the lung
258 has been already reported as an important mechanism in VILI (11). Cell phenotype changes included
259 Gr1 overexpression by alveolar macrophages, and CD62L overexpression by pulmonary monocytes.
260 Gr1 overexpression is the witness of an activation of macrophages, and has already been demonstrated
261 in infectious circumstances (36). Besides, CD62L is an adhesion molecule whose overexpression on
262 pulmonary monocytes has already been observed during mechanical ventilation and explained by
263 cellular activation related to stretch (12). We postulate that inflammatory response to mechanical
264 ventilation in Elastase mice could be related to pre-existing inflammation reflected by the presence of
265 activated alveolar macrophages CD11b^{mid}, and not to altered cellular mechanical properties
266 secondary to parenchymal destruction. Indeed, although morphological and functional lung
267 modifications were similar in Elastase mice at D14 and D21 as compared to Saline animals, no
268 modification in both proportions and activation state of pulmonary inflammatory cells was seen in
269 Elastase mice at D21. Previous data have already demonstrated the early and central role of activation

270 of alveolar macrophages subjected to stretch in the initiation of the inflammatory response to
271 mechanical ventilation (13). Pre-existing macrophage activation could predispose these cells to
272 further activation by mechanical ventilation. Whatever the underlining molecular mechanism, this
273 pulmonary inflammatory response following mechanical ventilation could play a deleterious role in
274 the progression of pulmonary emphysema, through a worsening of lung inflammation level (30,37).
275 Our study had some limitations. First we did not identify any substantial variations in inflammatory
276 cell populations in total lung in Saline mice after normal Vt mechanical ventilation, unlike a previous
277 study with a very close experimental protocol, which highlighted increased number of neutrophils in
278 total lung, and increased expression of CD62L on pulmonary monocytes, in response to normal Vt
279 mechanical ventilation in healthy mice (12). However, we observed a trend towards an increased
280 percentage of neutrophils and expression of CD62L on lung monocytes of Saline MV mice as
281 compared to Saline SV mice. The nature of our control group may explain this lack of significance.
282 Indeed, the Saline SV group (consisting of mice instilled with saline, anesthetized, intubated and
283 maintained in spontaneous ventilation for two hours) was probably subjected to some level of
284 aggression, including pulmonary micro-atelectasis due to hypoventilation. Second, we did not use an
285 infectious challenge (e.g., lipopolysaccharide instillation) in conjunction with elastase instillation and
286 mechanical ventilation. Such a triple hit model may be closer to the frequent clinical scenario of
287 COPD patients requiring mechanical ventilation because of pneumonia, but its implementation and
288 interpretation may be complex.

289

290 **CONCLUSION**

291

292 In conclusion, in a murine model of pulmonary emphysema induced by tracheal instillation of
293 elastase, inflammatory response to normal Vt mechanical ventilation was characterized by an increase
294 in the proportion of pulmonary neutrophils and an activation of alveolar macrophages and pulmonary

295 monocytes. This response was observed only when the emphysema model showed an underlying
296 inflammation, reflected by the presence of activated alveolar macrophages CD11b^{mid}.

297

298 TABLES AND FIGURES LEGENDS

299

300 **Figure 1.** Experimental design. C57BL/6 mice received a tracheal instillation of either elastase
301 (Elastase mice) or saline (Saline mice). After 14 (A) or 21 (B) days, mice were anesthetized, intubated
302 and subjected to either spontaneous ventilation (SV mice) or mechanical ventilation (MV mice), then
303 sacrificed after two hours.

304

305 **Figure 2.** Flow cytometric analysis of different inflammatory cell populations in mouse lungs. **A.** Dot-
306 plot showing side-scatter (SS) versus forward-scatter (FS) within total cell population. Cellular debris
307 and lymphocyte were excluded from the analysis. Myeloid cells were gated (G1) on compatible size
308 (FS) and granularity (SS). **B.** Dot-plot showing FS versus pulse width within G1 gated events.
309 Doublets and triplets were subtracted from cell analysis through a second gate (G2) defined on pulse
310 width, which distinguished cell aggregates from unique events (called singlets). From there, only
311 combined G1 and G2 gated events were analysed. **C.** Dot-plot showing CD11c versus CD11b
312 expression within combined G1 and G2 gated events. Alveolar macrophages were identified by
313 CD11c⁺ CD11b⁻ phenotype. Autofluorescence level was high in this cell population. **D.** Dot-plot SS
314 versus CD11b expression within combined G1 and G2 gated events. G3 gated CD11b⁺ cells with
315 neutrophils compatible granularity, G4 gated CD11b⁺ cells with monocytes compatible granularity.
316 **E.** Dot plot CD11c versus Gr1 expression within combined G1, G2 and G3 gated events. Neutrophils
317 were defined as CD11c⁻ Gr1⁺ cells. **F.** Dot plot CD11c versus Gr1 expression within combined G1,
318 G2 and G4 gated events. Monocytes were defined as CD11c⁻ Gr1^{mid} cells.

319

320 **Figure 3.** Morphometric analysis. **A, B, C.** Representative photomicrographs (50-fold magnification)
321 of histological slides of murine lungs. Hematoxylin-eosin staining. Saline SV mice, 21 days after
322 tracheal instillation of saline (A), Elastase SV mice, D14 (B), Elastase SV mice, D21 (C). **D.** Mean
323 chord length of alveoli in SV and MV mice, 21 days after saline tracheal instillation, 14 and 21 days
324 after elastase tracheal instillation. Values are expressed as medians \pm interquartile range. n = 4-5
325 animals /group. \pm and * denote Benjamini-Hochberg corrected p value <0.10 (marginally significant)
326 and <0.05 respectively for the following Mann-Whitney pairwise comparisons (following Kruskal-
327 Wallis test): Saline SV vs Saline MV, Saline SV vs Ela SV D14, Saline SV vs Ela SV D21, Saline MV
328 vs Ela MV D14, Saline MV vs Ela MV D21, Ela SV vs Ela MV D14, Ela SV vs Ela MV D21, Ela SV
329 D14 vs Ela SV D21, Ela MV D14 vs Ela MV D21. *Definition of abbreviations:* SV, spontaneous
330 ventilation; MV, mechanical ventilation; Ela, elastase tracheal instillation.

331

332 **Figure 4.** Evolution of dynamic compliance, calculated using the single frequency forced oscillation
333 technique, during two hours of mechanical ventilation in Saline and Elastase mice, at D14 (A) and
334 D21 (B) of tracheal instillation. Values are expressed as median \pm interquartile range. n = 6 animals
335 /group at D14, and 13 animals /group at D21. \pm , *, ** and *** denote p value <0.10 (marginally
336 significant), <0.05 , <0.01 and <0.001 respectively for the Mann-Whitney pairwise comparisons
337 (following Kruskal-Wallis test), Elastase MV versus Saline MV. *Definition of abbreviations:* MV,
338 mechanical ventilation; H0, at ventilator connection; H0', after volume history standardization; H1,
339 after one hour of MV; H2, at the end of MV.

340

341 **Figure 5.** Relative values of pulmonary inflammatory cell populations analyzed by flow cytometry on
342 total lung cell suspensions of mice subjected to spontaneous (SV) or mechanical (MV) ventilation 14
343 days after instillation of saline (Saline) or elastase (Ela), expressed as percentage of gated cells.
344 Values are expressed as median \pm interquartile range. n = 5 animals /group. \pm and * denote Benjamini-

345 Hochberg corrected p value <0.10 (marginally significant) and <0.05 respectively for the following
346 Mann-Withney pairwise comparisons (following Kruskal-Wallis test): Saline SV vs Saline MV,
347 Saline SV vs Ela SV, Ela SV vs Ela MV, Saline MV vs Ela MV. *Definition of abbreviations:* Ela,
348 Elastase; SV, spontaneous ventilation; MV, mechanical ventilation.

349

350 **Figure 6.** Activation markers of alveolar macrophages (A) and pulmonary monocytes (B), analyzed
351 by flow cytometry on total lung cell suspensions of mice subjected to spontaneous (SV) or mechanical
352 (MV) ventilation 14 days after instillation of saline (Saline) or elastase (Ela), expressed as mean
353 fluorescent intensity (MFI). **A.** CD11b and Gr1 expression, and autofluorescence of alveolar
354 macrophages. **B.** Gr1, CD11b and CD62L expression on pulmonary monocytes. Values are expressed
355 as median \pm interquartile range. n = 5 animals /group. [±] denotes Benjamini-Hochberg corrected p
356 value <0.10 (marginally significant) for the following Mann-Withney pairwise comparisons
357 (following Kruskal-Wallis test): Saline SV vs Saline MV, Saline SV vs Ela SV, Ela SV vs Ela MV,
358 Saline MV vs Ela MV. *Definition of abbreviations:* Ela, Elastase; SV, spontaneous ventilation; MV,
359 mechanical ventilation.

360

361 **TABLE 1. Respiratory mechanics data** during mechanical ventilation in D14 and D21 Saline and
362 Elastase mice.

363 Values are expressed as medians \pm interquartile range. n = 6 animals /group at D14, 13 animals /group
364 at D21. ^x, *, **, and **** denote p value <0.10 (marginally significant), <0.05, <0.01 and <0.001
365 respectively for the Mann-Withney pairwise comparisons (following Kruskal-Wallis test), Elastase
366 MV versus Saline MV. *Definition of abbreviations:* MV, mechanical ventilation; H0', after volume
367 history standardization consisting of three inflations to a transrespiratory pressure of 30 cmH₂O; H1,
368 after one hour; H2, at the end of MV; Ppeak, peak airway pressure; Pmean, mean airway pressure;
369 Compliance, Resistance, dynamic compliance and resistance of the respiratory system calculated

370 using the single frequency forced oscillation technique; Δ Compliance, percentage of compliance
371 decrease during mechanical ventilation, between H0' and H2.

372

373 **LIST OF ABBREVIATIONS**

374 BAL: Bronchoalveolar Lavage

375 COPD: Chronic Obstructive Lung Disease

376 FBS: Fetal Bovine Serum

377 ICU: Intensive Care Unit

378 MV: Mechanical Ventilation

379 Pmean: Mean Airway Pressure

380 Ppeak: Peak Airway Pressure

381 SV: Spontaneous Ventilation

382 VILI: Ventilator-Induced Lung Injury

383 Vt: Tidal Volume

384

385 **DECLARATIONS**

386 **Ethics approval**

387 All the experiments were performed in accordance with the official regulations of the French Ministry
388 of Agriculture and the US National Institute of Health guidelines for the experimental use of animals,
389 were approved by the local institutional animal care and use committee, and were conducted in a
390 specific “little animal” platform (Plateforme Exploration Fonctionnelle du Petit Animal, INSERM
391 U955, Créteil, France).

392 **Consent for publication**

393 Not applicable

394 **Availability of data and materials**

395 The datasets during and/or analysed during the current study available from the corresponding author
396 on reasonable request.

397 **Competing interests**

398 All the authors declare no competing interest in relation with this work.

399 **Funding**

400 No funding.

401 **Authors' contributions**

402 Study concept and design: AR, GV, EG, FR, DI, LB, BM, AMD, JB

403 Acquisition of data: AR, GV, EG, FR, JTVN

404 Analysis and interpretation of data: AR, GV, EG, FR, JTVN, BM, AMD, JB

405 Drafting of the manuscript: AR, GV, EG, AMD, JB

406 Critical revision of the manuscript for important intellectual content: all authors

407 Statistical analysis: AR, GV, AMD

408 Study supervision: GV, JB

409 All authors read and approved the final manuscript.

410 **Acknowledgments**

411 We are very grateful to the following members of U955 INSERM unit for their scientific and
412 technical assistance: Stéphane Kerbrat, Dr Sabine Le Gouvello, Dr Laurent Boyer (Equipe 4,
413 INSERM U955, Créteil), Rachid Souktani (Plateforme Exploration Fonctionnelle du Petit Animal,
414 INSERM U955, Créteil), Aurélie Guguin and Adeline Henri (Plateforme Cytométrie en Flux,
415 INSERM U955, Créteil), Xavier Decrouy (Plateforme Imagerie, INSERM U955 Créteil).

416

417 **REFERENCES**

418

- 419 1. Vestbo J, Hurd SS, Agustí AG, Jones PW, Vogelmeier C, Anzueto A, et al. Global strategy for the
420 diagnosis, management, and prevention of chronic obstructive pulmonary disease: GOLD
421 executive summary. *Am J Respir Crit Care Med.* 2013;187(4):347-65.
- 422 2. Molinari N, Briand C, Vachier I, Malafaye N, Aubas P, Georgescu V, et al. Hospitalizations for
423 COPD Exacerbations: Trends and Determinants of Death. *COPD.* 2015;12(6):621-7.
- 424 3. Ongel EA, Karakurt Z, Salturk C, Takir HB, Burunsuzoglu B, Kargin F, et al. How do COPD
425 comorbidities affect ICU outcomes? *Int J Chron Obstruct Pulmon Dis.* 2014;9:1187-96.
- 426 4. Webb HH, Tierney DF. Experimental pulmonary edema due to intermittent positive pressure
427 ventilation with high inflation pressures. Protection by positive end-expiratory pressure. *Am Rev
428 Respir Dis.* 1974;110(5):556-65.
- 429 5. Dreyfuss D, Basset G, Soler P, Saumon G. Intermittent positive-pressure hyperventilation with
430 high inflation pressures produces pulmonary microvascular injury in rats. *Am Rev Respir Dis.*
431 1985;132(4):880-4.
- 432 6. Dreyfuss D, Soler P, Basset G, Saumon G. High inflation pressure pulmonary edema. Respective
433 effects of high airway pressure, high tidal volume, and positive end-expiratory pressure. *Am Rev
434 Respir Dis.* 1988;137(5):1159-64.
- 435 7. Ventilation with lower tidal volumes as compared with traditional tidal volumes for acute lung
436 injury and the acute respiratory distress syndrome. The Acute Respiratory Distress Syndrome
437 Network. *N Engl J Med.* 2000;342(18):1301-8.
- 438 8. Malhotra A. Low-tidal-volume ventilation in the acute respiratory distress syndrome. *N Engl J
439 Med.* 2007;357(11):1113-20.
- 440 9. Halbertsma FJJ, Vaneker M, Scheffer GJ, van der Hoeven JG. Cytokines and biotrauma in
441 ventilator-induced lung injury: a critical review of the literature. *Neth J Med.*
442 2005;63(10):382-92.
- 443 10. Belperio JA, Keane MP, Burdick MD, Londhe V, Xue YY, Li K, et al. Critical role for CXCR2
444 and CXCR2 ligands during the pathogenesis of ventilator-induced lung injury. *J Clin Invest.*
445 2002;110(11):1703-16.
- 446 11. Choudhury S, Wilson MR, Goddard ME, O'Dea KP, Takata M. Mechanisms of early pulmonary
447 neutrophil sequestration in ventilator-induced lung injury in mice. *Am J Physiol Lung Cell Mol
448 Physiol.* 2004;287(5):L902-910.
- 449 12. Wilson MR, O'Dea KP, Zhang D, Shearman AD, van Rooijen N, Takata M. Role of lung-
450 margined monocytes in an in vivo mouse model of ventilator-induced lung injury. *Am J Respir
451 Crit Care Med.* 2009;179(10):914-22.
- 452 13. Frank JA, Wray CM, McAuley DF, Schwendener R, Matthay MA. Alveolar macrophages
453 contribute to alveolar barrier dysfunction in ventilator-induced lung injury. *Am J Physiol Lung
454 Cell Mol Physiol.* 2006;291(6):L1191-1198.

- 455 14. Wolthuis EK, Vlaar APJ, Choi G, Roelofs JJTH, Juffermans NP, Schultz MJ. Mechanical
456 ventilation using non-injurious ventilation settings causes lung injury in the absence of pre-
457 existing lung injury in healthy mice. *Crit Care*. 2009;13(1):R1.
- 458 15. Vaporidi K, Voloudakis G, Priniannakis G, Kondili E, Koutsopoulos A, Tsatsanis C, et al. Effects
459 of respiratory rate on ventilator-induced lung injury at a constant PaCO₂ in a mouse model of
460 normal lung. *Crit Care Med*. 2008;36(4):1277-83.
- 461 16. Dreyfuss D, Soler P, Saumon G. Mechanical ventilation-induced pulmonary edema. Interaction
462 with previous lung alterations. *Am J Respir Crit Care Med*. 1995;151(5):1568-75.
- 463 17. Yoshida T, Tuder RM. Pathobiology of cigarette smoke-induced chronic obstructive pulmonary
464 disease. *Physiol Rev*. 2007;87(3):1047-82.
- 465 18. Abboud RT, Vimalanathan S. Pathogenesis of COPD. Part I. The role of protease-antiprotease
466 imbalance in emphysema. *Int J Tuberc Lung Dis*. 2008;12(4):361-7.
- 467 19. Angelis N, Porpodis K, Zarogoulidis P, Spyrtos D, Kioumis I, Papaiwannou A, et al. Airway
468 inflammation in chronic obstructive pulmonary disease. *J Thorac Dis*. 2014;6(Suppl 1):S167-72.
- 469 20. Kaplan PD, Kuhn C, Pierce JA. The induction of emphysema with elastase. I. The evolution of the
470 lesion and the influence of serum. *J Lab Clin Med*. 1973;82(3):349-56.
- 471 21. Houghton AM, Quintero PA, Perkins DL, Kobayashi DK, Kelley DG, Marconcini LA, et al.
472 Elastin fragments drive disease progression in a murine model of emphysema. *J Clin Invest*.
473 2006;116(3):753-9.
- 474 22. Tasaka S, Inoue K-I, Miyamoto K, Nakano Y, Kamata H, Shinoda H, et al. Role of interleukin-6
475 in elastase-induced lung inflammatory changes in mice. *Exp Lung Res*. 2010;36(6):362-72.
- 476 23. Plantier L, Marchand-Adam S, Antico Arciuch VG, Antico VG, Boyer L, De Coster C, et al.
477 Keratinocyte growth factor protects against elastase-induced pulmonary emphysema in mice. *Am*
478 *J Physiol Lung Cell Mol Physiol*. 2007;293(5):L1230-1239.
- 479 24. Mekontso Dessap A, Voirit G, Zhou T, Marcos E, Dudek SM, Jacobson JR, et al. Conflicting
480 physiological and genomic cardiopulmonary effects of recruitment maneuvers in murine acute
481 lung injury. *Am J Respir Cell Mol Biol*. 2012;46(4):541-50.
- 482 25. Gonzalez-Juarrero M, Shim TS, Kipnis A, Junqueira-Kipnis AP, Orme IM. Dynamics of
483 macrophage cell populations during murine pulmonary tuberculosis. *J Immunol*.
484 2003;171(6):3128-35.
- 485 26. Brando B, Barnett D, Janossy G, Mandy F, Autran B, Rothe G, et al. Cytofluorometric methods
486 for assessing absolute numbers of cell subsets in blood. European Working Group on Clinical Cell
487 Analysis. *Cytometry*. 2000;42(6):327-46.
- 488 27. Mouded M, Egea EE, Brown MJ, Hanlon SM, Houghton AM, Tsai LW, et al. Epithelial cell
489 apoptosis causes acute lung injury masquerading as emphysema. *Am J Respir Cell Mol Biol*.
490 2009;41(4):407-14.
- 491 28. Wright JL, Cosio M, Churg A. Animal models of chronic obstructive pulmonary disease. *Am J*
492 *Physiol Lung Cell Mol Physiol*. 2008;295(1):L1-15.

- 493 29. Aida Y, Shibata Y, Abe S, Inoue S, Kimura T, Igarashi A, et al. Inhibition of elastase-pulmonary
494 emphysema in dominant-negative MafB transgenic mice. *Int J Biol Sci.* 2014;10(8):882-94.
- 495 30. Woodruff PG, Koth LL, Yang YH, Rodriguez MW, Favoreto S, Dolganov GM, et al. A
496 distinctive alveolar macrophage activation state induced by cigarette smoking. *Am J Respir Crit
497 Care Med.* 2005;172(11):1383-92.
- 498 31. Domagała-Kulawik J, Maskey-Warzechowska M, Hermanowicz-Salamon J, Chazan R.
499 Expression of macrophage surface markers in induced sputum of patients with chronic obstructive
500 pulmonary disease. *J Physiol Pharmacol.* 2006;57 Suppl 4:75-84.
- 501 32. Sköld CM, Eklund A, Halldén G, Hed J. Autofluorescence in human alveolar macrophages from
502 smokers: relation to cell surface markers and phagocytosis. *Exp Lung Res.* 1989;15(6):823-35.
- 503 33. Gajic O, Dara SI, Mendez JL, Adesanya AO, Festic E, Caples SM, et al. Ventilator-associated
504 lung injury in patients without acute lung injury at the onset of mechanical ventilation. *Crit Care
505 Med.* 2004;32(9):1817-24.
- 506 34. Allen GB, Suratt BT, Rinaldi L, Petty JM, Bates JHT. Choosing the frequency of deep inflation in
507 mice: balancing recruitment against ventilator-induced lung injury. *Am J Physiol Lung Cell Mol
508 Physiol.* 2006;291(4):L710-717.
- 509 35. Martin EL, Truscott EA, Bailey TC, Leco KJ, McCaig LA, Lewis JF, et al. Lung mechanics in the
510 TIMP3 null mouse and its response to mechanical ventilation. *Exp Lung Res.* 2007;33(2):99-113.
- 511 36. Mordue DG, Sibley LD. A novel population of Gr-1+-activated macrophages induced during
512 acute toxoplasmosis. *J Leukoc Biol.* 2003;74(6):1015-25.
- 513 37. Perez T, Mal H, Aguilaniu B, Brillet P-Y, Chaouat A, Louis R, et al. [COPD and inflammation:
514 statement from a French expert group. Phenotypes related to inflammation]. *Rev Mal Respir.*
515 2011;28(2):192-215.

516

FIGURE 1

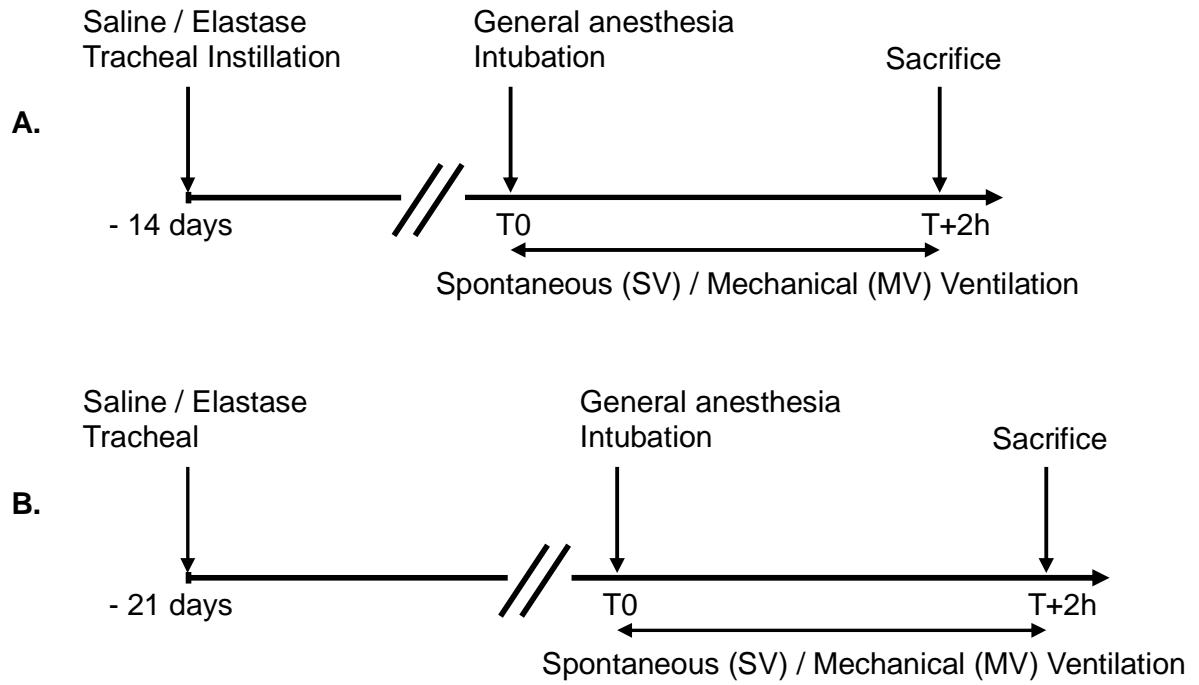


FIGURE 2

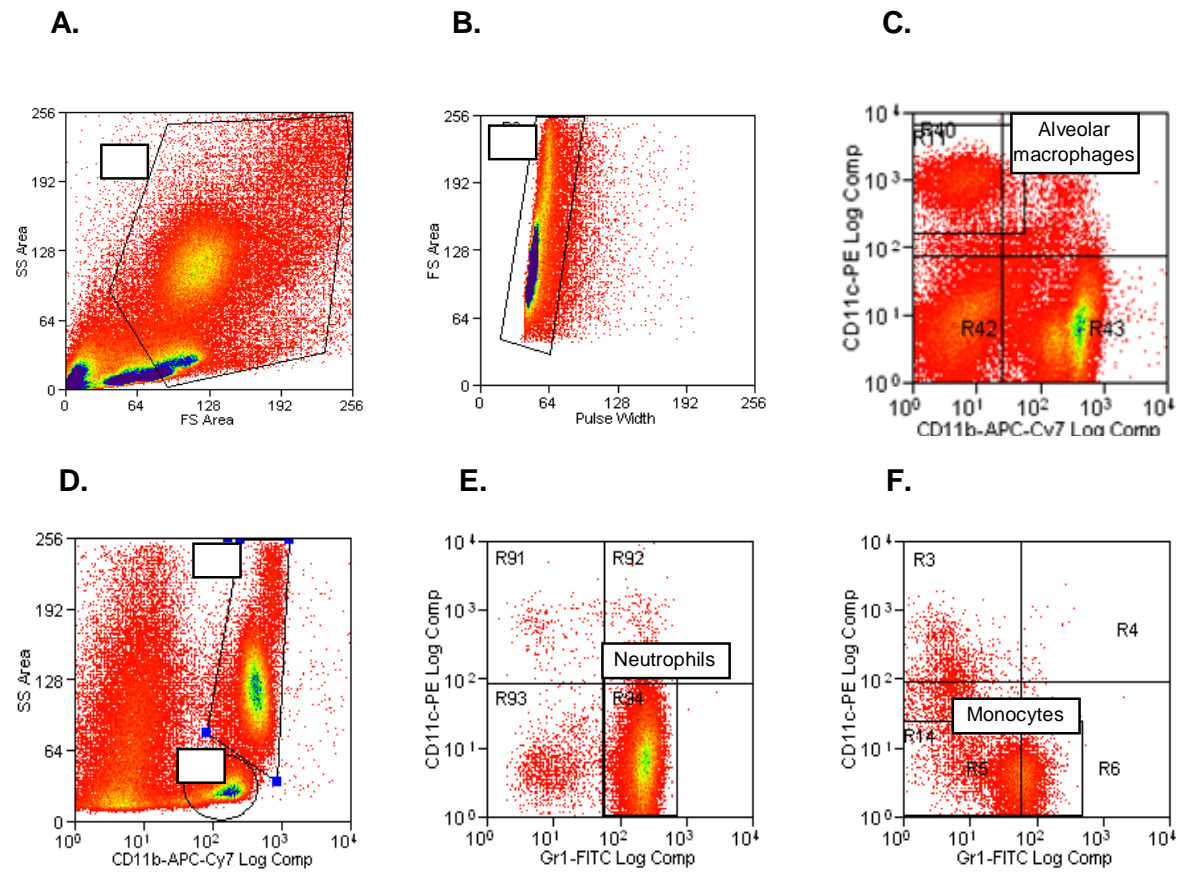


FIGURE 3

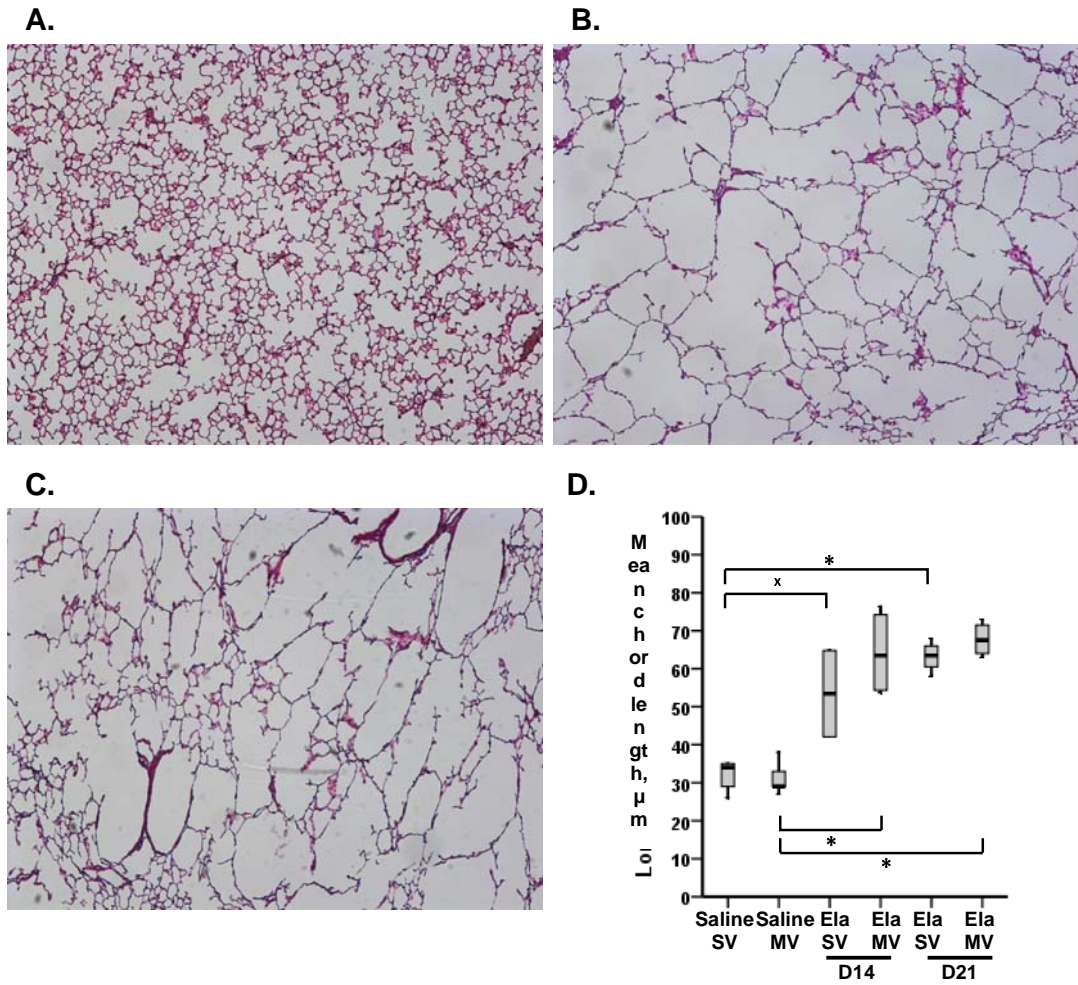


FIGURE 4

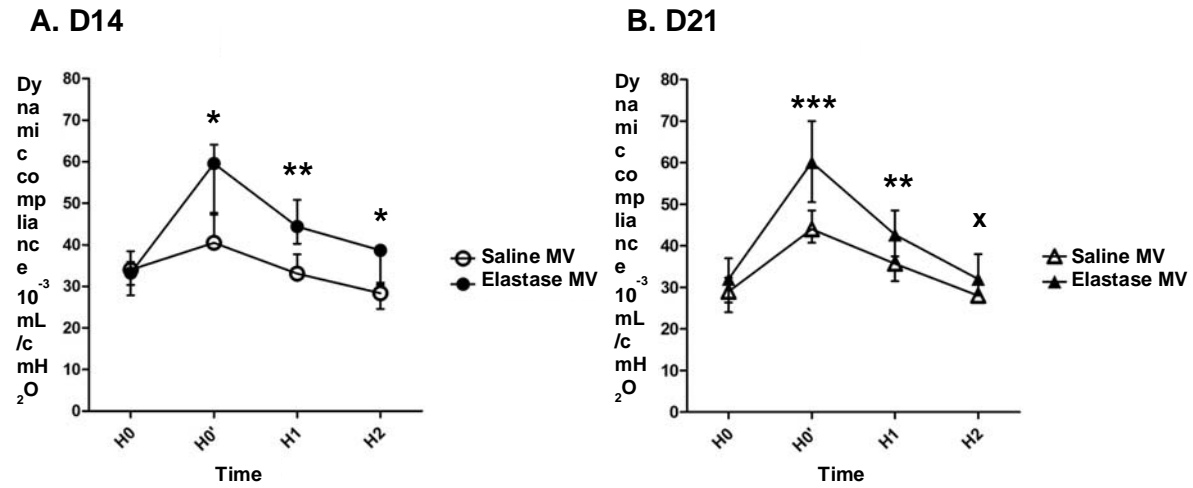


FIGURE 5

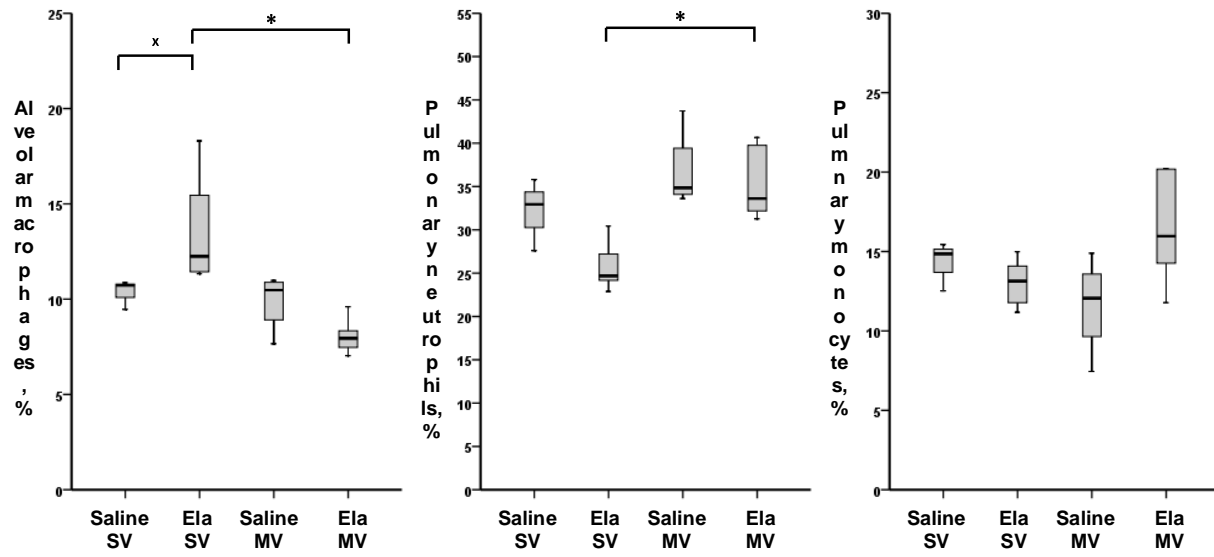


FIGURE 6

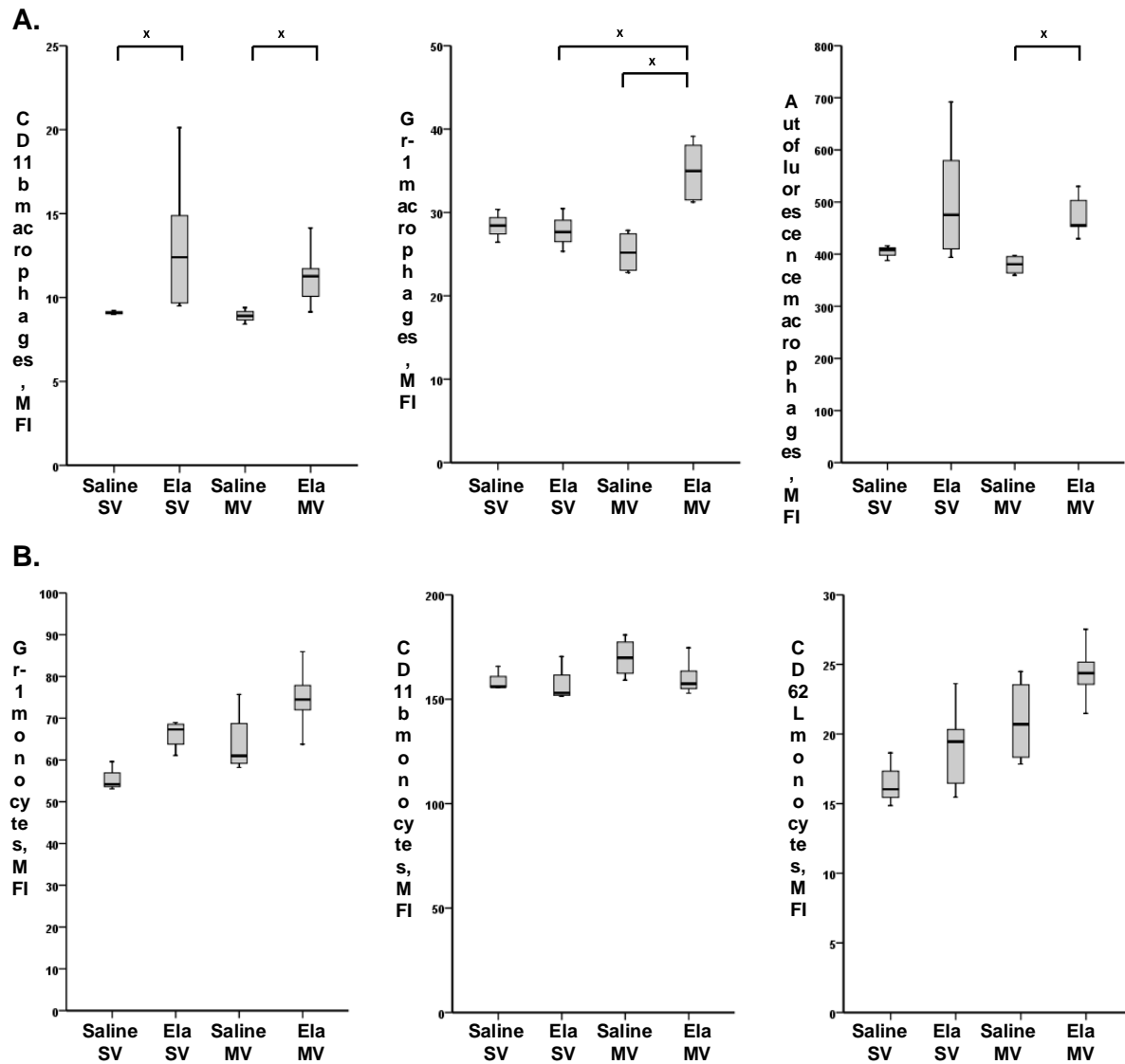


TABLE 1. Respiratory mechanics data during mechanical ventilation in D14 and D21 Saline and Elastase mice.

	Saline MV			Elastase MV		
	H0'	H1	H2	H0'	H1	H2
D14						
Ppeak , cmH2O	9.4±0.9	10.5±1.2	11.2±1.7	7.9±1.3*	8.4±1.0*	9.3±1.8*
Pmean , cmH2O	6.3±0.3	6.9±0.7	7.4±0.9	6.0±0.4	6.2±0.4 ^x	6.5±0.8*
Compliance , 10 ⁻³ mL/cmH2O	41.0±8.0	33.0±6.0	28.0±6.0	62.0±13.0*	46.0±11.0**	39.0±10.0*
Resistance , 10 ⁻² cmH2O.s/mL	70.0±21.0	75.0±23.0	72.0±26.0	72.0±8.0	80.0±11.0	79.0±9.0
ΔCompliance , %			-33.3±9.6			-39.1±4.3 ^x
D21						
Ppeak , cmH2O	8.7±1.0	9.8±0.9	10.7±1.0	8.0±0.7**	8.7±1.1**	9.8±1.9
Pmean , cmH2O	6.3±0.9	6.8±0.8	7.2±0.7	6.1±0.6	6.2±0.7**	6.5±0.7 ^x
Compliance , 10 ⁻³ mL/cmH2O	44.0±8.0	36.0±6.0	28.0±4.0	60.0±20.0***	43.0±12.0**	32.0±10.0 ^x
Resistance , 10 ⁻² cmH2O.s/mL	69.0±17.0	79.0±19.0	77.0±12.0	76.0±12.0**	76.0±23.0	88.0±20.0
ΔCompliance , %			-34.3±6.4			-40.8±14.8*

Values are expressed as medians ± interquartile range. n = 6 animals /group at D14, 13 animals /group at D21. ^x, *, ** and *** denote p value <0.10 (marginally significant), <0.05, <0.01 and <0.001 respectively for the Mann-Whitney pairwise comparisons (following Kruskal-Wallis test), Elastase MV *versus* Saline MV. *Definition of abbreviations*: MV, mechanical ventilation; H0', after volume history standardization consisting of three inflations to a transrespiratory pressure of 30 cmH₂O; H1, after one hour; H2, at the end of MV; Ppeak, peak airway pressure; Pmean, mean airway pressure; Compliance, Resistance, dynamic compliance and resistance of the respiratory system calculated using the single frequency forced oscillation technique; ΔCompliance, percentage of compliance decrease during mechanical ventilation, between H0' and H2.